Theory of the Greenspan viscometer

Keith A. Gillis,* James B. Mehl,† and Michael R. Moldover‡
Process Measurements Division, National Institute of Standards and Technology, Gaithersburg, Maryland 20899-8360, U.S.A.
(Dated: November 11, 2002)

We present an acoustic model of the Greenspan acoustic viscometer, a practical instrument for accurately measuring the viscosity η of gases. As conceived by Greenspan, the viscometer is a Helmholtz resonator composed of two chambers coupled by a duct of radius r_d. In the lowest order, $\eta = \pi f \rho (r_d/Q)^2$, where f and Q are the frequency and quality factor of the isolated Greenspan mode, and ρ is the gas density. Thus the viscosity can be determined without calibration by measuring the duct radius and frequency response of the resonator. In the full acoustic model of the resonator, the duct is represented by a T-equivalent circuit, the chambers as lumped impedances, and the effects of the diverging fields at the duct ends by lumped end impedances with inertial and resistive components. The model accounts for contributions to $1/Q$ from thermal dissipation (primarily localized in the chambers) and from a judiciously-located capillary used for filling and evacuating the resonator. A robust, prototype instrument is being used for measuring the viscosity of reactive gases used in semiconductor processing. For well-characterized surrogate gases, the prototype viscometer generated values of η that were within $\pm 0.8\%$ of published reference values throughout the pressure range 0.2–3.2 MPa.

I. INTRODUCTION

As conceived by Greenspan,[1] the acoustic viscometer is a Helmholtz resonator composed of two gas-filled chambers connected by a duct of radius r_d. (See Fig 1.) By design, the radius of the duct is much smaller than its length L_d and smaller than the dimensions of the chambers (radius r_c, length L_c). Such a resonator has a low frequency (Greenspan) mode in which the gas oscillates between the chambers through the duct. It is easy to measure the frequency response of the Greenspan mode very accurately because it is well below the frequencies of all other acoustic modes of the enclosed gas and the elastic modes of the resonator body. The damping of the Greenspan mode is determined primarily by the viscosity of the gas η; in the lowest order, $\eta = \pi f \rho (r_d/Q)^2$, where f and Q are the frequency and quality factor of the mode and ρ is the gas density. The objective of this paper is to calculate an accurate response function so that the Greenspan viscometer can be used to determine accurately the viscosity of gases.

Ultimately, we are concerned with the viscosity of the highly reactive gases used in semiconductor processing. The data are needed to calibrate mass-flow controllers and to model processes such as chemical vapor deposition. Also, the viscosity of helium-argon and helium-xenon mixtures is needed to optimize thermoacoustic machinery. Below, we provide test results from a prototype Greenspan viscometer using five well-studied surrogate gases over the pressure range 0.2–3.2 MPa. The resulting values of η were within $\pm 0.8\%$ of published reference values.

Figure 1 shows the Greenspan viscometer described by Wilhelm *et al.*[2–4] (An earlier version of the viscometer and additional experimental detail appear in Ref 5.) Two right-circular cylindrical chambers coupled by a concentric cylindrical duct form a resonator whose low-frequency mode consists of oscillatory gas flow between the chambers (assumed to be of equal volume). The "mass element" of the resonator is the cylindrical mass of gas in the duct and near the duct ends. It has a nearly uniform flow velocity and effective mass $A_d(L_d + 2\delta_i)\rho$, where ρ is the gas density, $A_d = \pi r_d^2$ is the cross-sectional area of the duct, L_d is the duct length, and the length $\delta_i \approx 0.655 \cdot r_d$ is an inertial end correction which accounts for diverging flow at the duct ends. Flow into a chamber increases the pressure in that chamber and provides

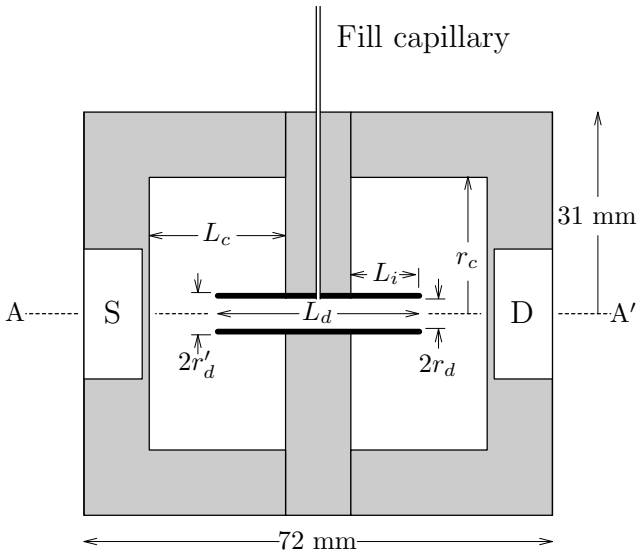

FIG. 1: Cross section of a Greenspan viscometer. The dotted line AA′ indicates the axis of circular symmetry for all parts except the fill capillary. Two cylindrical chambers fitted with source (S) and detector (D) transducers are coupled by a concentric cylindrical duct. The dimensions in millimeters are $L_d = 31.17$, $r_d = 2.316$, $r'_d = 3.21$, $r_c = 21.02$, $L_c = 21.04$, and $L_i = 10.5$. The fill capillary has an inner radius $r_f = 0.10$ mm (not to scale) and a length $L_f = 800$ mm. As shown, it is attached at the center of the duct.

a restoring force; the effective force constant is $\rho c^2 A_d^2/V_c$ per chamber, where c is the speed of sound and V_c is the volume of a single chamber. A zero-order estimate of the frequency $\omega_0 = ck_0$ is

$$k_0^2 = \frac{2A_d}{V_c(L_d + 2\delta_i)}. \tag{1}$$

(If the chambers have unequal volumes V_1 and V_2, $2/V_c$ should be replaced by $1/V_1 + 1/V_2$.) For the resonator in Fig 1, Eq (1) has a numerical value $k_0 \approx 5.8$ m^{-1}. The corresponding frequency is a few hundred Hz for typical gases, well below the frequencies of elastic vibrations of the resonator body and higher acoustic modes of the gas in the resonator. Thus, the Helmholtz mode is isolated and non-degenerate, which is desirable if η is to be determined with the highest accuracy from measurements of the mode's resonance profile.

In addition, the low frequency of the Greenspan mode means that the corresponding wavelength is much larger than the viscous and thermal penetration lengths δ_v and δ_t. In this limit the equations for dissipative acoustic flow in a duct have a relatively simple form. Also, the lengths δ_v and δ_t are much larger than the mean free path in the gas, so inertial and thermal accommodation effects in the boundary conditions can be neglected.

In the remainder of this section, we describe the principle of the measurement by considering the viscous and other contributions to the inverse quality factor $(1/Q)$ of the resonator. In section II, we develop a full acoustic model to predict the frequency response of the resonator, from which the viscosity is deduced.

Acoustic energy dissipation in the gas is a result of both surface phenomena (energy transport near the resonator wall) and volume phenomena (energy transport far from the wall). At low frequencies and at pressures in the range 0.1 MPa to 3 MPa, the main sources of dissipation for non-relaxing gases are viscous and thermal boundary layer phenomena, which can be estimated using the formulae derived by Morse and Ingard for flat surfaces.[6] The rate of energy loss within the viscous boundary layers in the duct is

$$\dot{E}_v = -\frac{1}{2}\rho\omega\delta_v u_d^2 \cdot 2\pi r_d(L_d + 2\epsilon_r r_d). \tag{2}$$

Here $\delta_v = \sqrt{2D_v/\omega}$, where $D_v = \eta/\rho$ is the viscous diffusivity, u_d is the rms value of the gas velocity in the duct and $\epsilon_r r_d$ is an effective length associated with viscous dissipation at the duct ends. The rate of energy loss within the thermal boundary layer in the chambers is

$$\dot{E}_t = -\frac{(\gamma-1)\omega\delta_t}{2\rho c^2} p_{ch}^2 \cdot 2S_c, \tag{3}$$

where $\gamma = C_p/C_v$ is the ratio of the specific heat per unit mass at constant pressure to the specific heat per unit mass at constant volume, $\delta_t = \sqrt{2D_t/\omega}$ is the thermal penetration length (D_t is the thermal diffusivity), p_{ch} is the rms pressure amplitude in the chambers and S_c is the total surface area within one chamber. The total acoustic energy in the resonator is

$$E \approx \rho u_d^2 \cdot A_d(L_d + 2\delta_i) \approx \frac{p_{ch}^2}{\rho c^2} \cdot 2V_c. \tag{4}$$

Acoustic dissipation within the resonator volume is important for gases at very low density, gases near the liquid-vapor critical point, and relaxing gases under a wide range of conditions. The fractional rate of energy loss due to these processes is

$$\frac{\dot{E}_{\text{volume}}}{E} = -\frac{\omega^2}{c^2}\left[\frac{4}{3}D_v + (\gamma-1)D_t + \frac{\eta_b}{\rho}\right]. \tag{5}$$

The first two terms in Eq (5) are the classical absorption terms. The third term describes absorption due to relaxation processes and is characterized by the bulk viscosity η_b. Relaxation processes govern the energy exchange between translational degrees of freedom (the acoustic mode) and other internal modes of the fluid, such as molecular vibrations, metastable intermolecular bound states, or critical fluctuations. If the process can be characterized by a single relaxation time τ_{relax}, then the bulk viscosity is approximately

$$\eta_b = (\gamma-1)\rho c^2 \frac{C_{\text{relax}}}{C_p} \frac{\tau_{\text{relax}}}{1 + (\omega\tau_{\text{relax}})^2}. \tag{6}$$

The inverse resonance quality factor $1/Q = -\dot{E}/(\omega E)$ is the sum of three terms:[7]

$$\frac{1}{Q} = \frac{1}{Q_v} + \frac{1}{Q_t} + \frac{1}{Q_{\text{volume}}} \tag{7}$$

$$\frac{1}{Q_v} = \frac{\delta_v}{r_d} \cdot \frac{L_d + 2\epsilon_r r_d}{L_d + 2\delta_i} \tag{8}$$

$$\frac{1}{Q_t} = \frac{(\gamma-1)\delta_t S_c}{2V_c} \tag{9}$$

$$\frac{1}{Q_{\text{volume}}} = \frac{\omega^2}{2c^2}\left[\frac{4}{3}\delta_v^2 + (\gamma-1)\delta_t^2 + \frac{2\eta_b}{\rho\omega}\right]. \tag{10}$$

If end effects are neglected, $1/Q_v$ is simply δ_v/r_d. For the resonator in Fig 1, the numerical value of ϵ_r is approximately 0.95 under typical experimental conditions, so the dissipative end effect acts to increase the viscous dissipation by an amount $2\epsilon_r r_d/L_d \approx 0.14$. The inertial end effect acts to increase the kinetic energy and hence decreases $1/Q_v$ by an amount $2\delta_i/L_d \approx 0.097$. Together, the inertial and dissipative end effects in the resonator contribute a net increase in $1/Q_v$ by a factor of 1.04.

Equation (7) shows that when thermal boundary layer and bulk absorption can be neglected, the viscosity can be determined as

$$\eta = \frac{1}{2}\omega\rho\delta_v^2 = \frac{\pi f \rho r_d^2}{Q^2}\left(\frac{L_d + 2\delta_i}{L_d + 2\epsilon_r r_d}\right)^2 \tag{11}$$

provided that the end corrections are known. The only requirements to measure f and Q are transducers that

(1) have a smooth frequency response (no sharp peaks) in the vicinity of the Helmholtz mode and (2) are stable during the few minutes required to measure the frequency response of the Helmholtz mode. The quality factor should be small enough so that $1/Q$ can be measured accurately but not so small that signal/noise is seriously degraded. In practice, these considerations lead to designs that work in the range $20 < Q < 100$.

For chambers with equal radii and lengths ($r_c = L_c$), the ratio V_c/S_c in Eq (7) is $r_c/4$. Because the penetration lengths δ_v and δ_t in gases are typically of the same magnitude, the desired dominance of the viscous term in Eq (7) requires $r_d \ll \frac{1}{2} r_c/(\gamma - 1)$. An attempt to satisfy this criterion drives the design toward cumbersome large chambers, low frequencies, and low Qs, where measurements become difficult. Thus, for the practical, compact acoustic viscometer shown in Fig 1, the thermal diffusivity contribution to Eq (11) must be estimated. At 300 K and 0.2 MPa the thermal term is 18% of the viscous term for argon and 4% for propane. Also, the advantages of a reasonably compact resonator require a duct of moderate length, so that end corrections are not negligible, so it is necessary to determine the parameter ϵ_r either through calculation or experiment.

II. ACOUSTIC MODEL OF THE RESONATOR

A. Acoustic propagation in a circular duct

Acoustic waves in gas-filled ducts are governed by the equations first proposed by Kirchhoff,[8] whose classic paper includes a description of the effects of the coupled acoustic, thermal, and vorticity waves in ducts of circular cross section. The low-frequency limit of his solutions, in a form appropriate for this paper, is generally attributed to Crandall.[9] We assume an implicit time dependence of all "small" acoustic quantities proportional to $e^{i\omega t}$ in the following. The acoustic pressure and volume velocity U are related by the transmission line equations

$$\frac{\partial p}{\partial z} = -\mathcal{Z} U, \quad \frac{\partial U}{\partial z} = -\mathcal{Y} p, \tag{12}$$

where $\mathcal{Z}$ is the series impedance and $\mathcal{Y}$ is the parallel admittance. For a circular duct in the low-frequency limit, these quantities are

$$\mathcal{Z} = \frac{i\omega\rho}{A_d} \frac{1}{1 - \mathbf{F}_v}, \quad \mathcal{Y} = \frac{i\omega A_d}{\rho c^2}[1 + (\gamma - 1)\mathbf{F}_t], \tag{13}$$

where $\mathbf{F}_v$ and $\mathbf{F}_t$ are defined by

$$\mathbf{F}_x = \frac{2J_1(\kappa_x r_d)}{\kappa_x r_d J_0(\kappa_x r_d)} \tag{14}$$

in terms of the Bessel functions $J_m(\zeta)$ and the parameters $\kappa_v = (1 - i)/\delta_v$ and $\kappa_t = (1 - i)/\delta_t$.

Elimination of U from Eq (12) yields

$$\frac{\partial^2 p}{\partial z^2} = \mathcal{Z}\mathcal{Y} p = \mathbf{\Gamma}^2 p, \tag{15}$$

where $\mathbf{\Gamma} = \sqrt{\mathcal{Z}\mathcal{Y}}$ is the propagation parameter for waves along the duct. Waves propagating in the $\pm z$ directions have a z-dependence proportional to $e^{\pm \mathbf{\Gamma} z}$. It follows that

$$U = \pm \frac{\mathbf{\Gamma}}{\mathcal{Z}} p = \pm \frac{\mathcal{Y}}{\mathcal{Z}} p = \pm \frac{p}{\mathbf{Z}_0}, \tag{16}$$

where $\mathbf{Z}_0 = \sqrt{\mathcal{Z}/\mathcal{Y}}$ is the characteristic impedance. By analogy with microwave circuit theory,[10] a duct of length L_d can be replaced by a T-equivalent circuit. Figure 2 shows the equivalent circuit of the viscometer duct terminated by the impedances associated with end effects and chambers (as defined in the next section). The

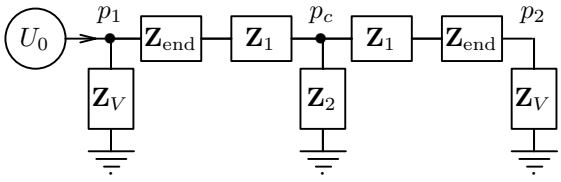

FIG. 2: Simplified equivalent circuit of the Greenspan viscometer.

impedances used to represent the duct are

$$\begin{aligned} \mathbf{Z}_1 &= \mathbf{Z}_0 \tanh(\mathbf{\Gamma} L_d/2) \\ &= \frac{i\omega\rho L_d}{2A_d(1 - \mathbf{F}_v)} \frac{\tanh(\frac{1}{2}\mathbf{\Gamma} L_d)}{\frac{1}{2}\mathbf{\Gamma} L_d} \end{aligned} \tag{17}$$

$$\begin{aligned} \mathbf{Z}_2 &= \frac{\mathbf{Z}_0}{\sinh(\mathbf{\Gamma} L_d)} \\ &= \frac{\rho c^2}{i\omega A_d L_d[1 + (\gamma - 1)\mathbf{F}_t]} \frac{\mathbf{\Gamma} L_d}{\sinh(\mathbf{\Gamma} L_d)}. \end{aligned} \tag{18}$$

In each case, the second form involves the ratio of a hyperbolic function to its argument, ratios which approach unity at zero frequency.

B. Lumped-component model

Lumped component acoustic models have been used for analyzing experimental results.[2–5] The use of such models is supported by numerical calculations,[11] which show that the pressure field within each chamber is spatially uniform except for entrance effects at the duct ends. The entrance effects are confined to a region whose dimensions are of order r_d. The effects of the chambers can be represented as a volume impedance in series with an end-effects term. Within the chambers the gas compressibility is isothermal at the walls and adiabatic far from the walls. An expression for the chamber impedance obtained by calculating the average compressibility within the chamber is

$$\mathbf{Z}_V = \frac{\rho c^2}{i\omega[V_c + \frac{1}{2}(1 - i)(\gamma - 1)S_c\delta_t]} = \frac{\rho c^2}{i\omega \mathbf{V}_c}, \tag{19}$$

where a complex volume $\mathbf{V}_c$ has been introduced in the second form for brevity. The ratio $S_c\delta_t/V_c$ is the approximate fraction of the chamber's volume in which the compressibility differs from the adiabatic value and where dissipation occurs.

The localized impedance at the duct ends can be written

$$\mathbf{Z}_{\rm end} = \frac{\rho\omega}{A_d}(i\delta_I + \delta_R), \tag{20}$$

where δ_I and δ_R are lengths which have been evaluated numerically.[11] To first order in δ_v the lengths are

$$\delta_I = \delta_i + \epsilon_i\delta_v, \quad \delta_R = \epsilon_r\delta_v. \tag{21}$$

As noted previously, for the experimental resonator, $\delta_i \approx 0.655\cdot r_d$; δ_I differs from this by a viscous boundary layer correction term and hence provides a more accurate representation of inertial end effects. When the duct ends are square, the techniques of Ref 11 predict a resistive parameter $\epsilon_{r0} \approx 0.987$. The boundary-layer approximation used in deriving this number breaks down when the tangential velocity varies rapidly on a length scale of order δ_v, as it does at the sharp corners of the duct ends where the acoustic velocity field is weakly divergent. Cutting off the singular integrals a distance of order δ_v from the sharp corners yields a fractional decrease in ϵ_r of order $(\delta_v/r_d)^{1/3}$. Recent numerical calculations[12] of the acoustic and vorticity fields near the duct end show that ϵ_r is slightly less than the constant term and varies weakly with δ_v/r_d according to

$$\epsilon_r \approx \epsilon_{r0} - 0.348(\delta_v/r_d)^{1/3} + 1.15(\delta_v/r_d). \tag{22}$$

The constant term in this expression is sensitive to the shape of the duct ends. Rounding the sharp edges decreases ϵ_r, and a slight burr can increase it. Improved agreement with experimental measurements in helium, for which the viscosity is known from first principles, was obtained by adjusting ϵ_{r0} to 1.024, a 3.7% increase. With this value of ϵ_{r0}, for the range $0.008 < \delta_v/r_d < 0.045$ that corresponds to recent experimental data, Eq (22) predicts values of ϵ_r varying from 0.96 to 0.95. Experimental evidence in support of the weak dependence on δ_v/r_d is included in Appendix A. In future work, we recommend rounding the corners of the duct ends to reduce the sensitivity of ϵ_r to δ_v/r_d.

The argument in Ref 11 that $\epsilon_i \approx \epsilon_r$ failed to take into account the directionality of the linear momentum, an effect that lowers the portion of ϵ_i associated with diverging flow outside the duct end by a small amount. The value $\epsilon_i \approx 0.86$ obtained in recent numerical work[12] is slightly smaller than ϵ_{r0}. Improved experimental agreement was obtained with a modest increase to $\epsilon_i \approx 0.96$.

As noted above, early viscometers used a fill capillary connected to one of the chambers, and the most recent version has a fill capillary attached to the main duct near its center. It is convenient to first consider a resonator without a fill capillary, as shown in Fig 2. Equation (18) shows that $\mathbf{Z}_2$ is proportional to the inverse duct volume, so it is much larger than $\mathbf{Z}_V$, which is proportional to the inverse chamber volume. Accordingly, forced acoustic flow will be mainly between the chambers with small perturbations due to the $\mathbf{Z}_2$ term.

The Greenspan viscometer has a low-frequency mode of odd symmetry which is completely independent of $\mathbf{Z}_2$. For this mode, the acoustic pressures in Fig 2 satisfy $p_2 = -p_1$ and $p_c = 0$. This will occur if the sum of the impedances in either leg of the "T" vanishes

$$\mathbf{Z}_1 + \mathbf{Z}_{\rm end} + \mathbf{Z}_V = 0. \tag{23}$$

This simplifies to

$$\frac{\omega^2}{c^2} = \frac{2A_d(1-\mathbf{F}_v)/\mathbf{V}_c}{L_d\tanh(\frac{1}{2}\mathbf{\Gamma}L_d)/(\frac{1}{2}\mathbf{\Gamma}L_d) + 2(\delta_I - i\delta_R)(1-\mathbf{F}_v)}. \tag{24}$$

In the absence of dissipative terms this agrees exactly with Eq (1), except for the hyperbolic-tangent term in the denominator. The magnitude of this term can be estimated by using $\mathbf{\Gamma} \approx i\omega/c \approx ik_0$, so that $(\mathbf{\Gamma}L_d)^2 \approx -2A_dL_d/V_c$, and

$$\frac{\tanh(\frac{1}{2}\mathbf{\Gamma}L_d)}{(\frac{1}{2}\mathbf{\Gamma}L_d)} \approx 1 + \frac{2A_dL_d}{3V_c}. \tag{25}$$

This differs from unity by 2/3 of the ratio of the duct volume to a chamber volume, or 1.2% for the experimental resonator. Terms like this are not negligible in the full model, but can be neglected in Eq (24) for present purposes. For small dissipation, neglecting terms of second order in δ_v and δ_t, approximating $\mathbf{F}_v$ by $(1-i)\delta_v/r_d$, and writing $\omega^2 \approx \omega_1^2(1+i/Q)$ where ω_1 is real, Eq (24) simplifies further to

$$\frac{\omega_1^2}{c^2}\left(1+\frac{i}{Q}\right) \approx k_0^2\left(1 + \frac{i}{Q_v} + \frac{i-1}{Q_t} - \frac{L_d + 2\epsilon_i r_d}{L_d + 2\delta_i}\frac{\delta_v}{r_d}\right). \tag{26}$$

The imaginary part of this equation is identical with the boundary-layer contributions to $1/Q$ in Eq (7); the real parts give an improved estimate of the resonance frequency.

When there is an acoustic source with volume velocity U_0 in chamber 1, the steady-state pressure in chamber 2 calculated from the equivalent circuit is

$$p_2 = \frac{\mathbf{Z}_V^2\mathbf{Z}_2U_0}{(\mathbf{Z}_1 + \mathbf{Z}_{\rm end} + \mathbf{Z}_V)(\mathbf{Z}_1 + \mathbf{Z}_{\rm end} + \mathbf{Z}_V + 2\mathbf{Z}_2)}, \tag{27}$$

which has the expected resonance term in the denominator. (The second factor in the denominator vanishes for the lowest plane-wave mode in the duct, with $kL_d \approx \pi$.)

C. Input impedance of fill capillary

The fill capillary is treated as a circular duct terminated by an impedance $\mathbf{Z}_{\rm t}$ (Fig 3). It has an input

impedance

$$\mathbf{Z}_{\rm in,fd} = \mathbf{Z}_{\rm ef1} + \mathbf{Z}_{\rm f1} + \frac{\mathbf{Z}_{\rm f2}(\mathbf{Z}_{\rm f1} + \mathbf{Z}_{\rm ef2})}{\mathbf{Z}_{\rm f2} + \mathbf{Z}_{\rm ef2} + \mathbf{Z}_{\rm f1}} \tag{28}$$

when the termination is open ($\mathbf{Z}_{\rm t} \approx 0$) and

$$\mathbf{Z}_{\rm in,fd} = \mathbf{Z}_{\rm ef1} + \mathbf{Z}_{\rm f1} + \mathbf{Z}_{\rm f2} \tag{29}$$

when the termination is closed. In these expressions the impedances $\mathbf{Z}_{\rm f1}$ and $\mathbf{Z}_{\rm f2}$ are defined by Eqs (17) and (18) with parameters appropriate for the fill capillary, *i.e.* $\mathbf{\Gamma} \to \mathbf{\Gamma}_f$, $L_d \to L_f$, and appropriate end corrections in Eq (20) are used for $\mathbf{Z}_{\rm ef1}$ and $\mathbf{Z}_{\rm ef2}$.

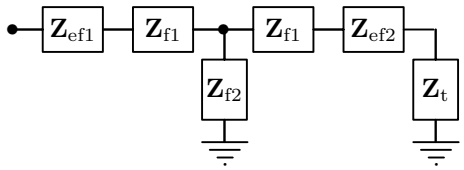

FIG. 3: Equivalent circuit of a fill capillary, treated as a circular duct terminated by an impedance $\mathbf{Z}_t$.

D. Fill capillary in chamber

Early versions of the viscometer[5] had a fill capillary in the source chamber. In this section, we derive the equation used for analyzing data taken with those viscometers, and show that it is difficult to minimize the effects of the fill capillary on the performance of the viscometer. These considerations led to relocating the fill capillary to the center of the duct.

The equivalent circuit of a resonator with a fill capillary in the source chamber can be obtained from Fig 2 by the introduction of $\mathbf{Z}_{\rm in,fd}$ in parallel with the left $\mathbf{Z}_V$. This parallel combination has an impedance

$$\mathbf{Z}'_V = \mathbf{Z}_V/(1 + \mathbf{Z}_V/\mathbf{Z}_{\rm in,fd}). \tag{30}$$

The equivalent circuit is no longer symmetric so the resonance condition is more complicated. With $\mathbf{Z}'_1 = \mathbf{Z}_1 + \mathbf{Z}_{\rm end}$, the resonance condition is

$$\mathbf{Z}'_V + \mathbf{Z}'_1 + \frac{\mathbf{Z}_2(\mathbf{Z}'_1 + \mathbf{Z}_V)}{\mathbf{Z}_2 + \mathbf{Z}'_1 + \mathbf{Z}_V} = 0, \tag{31}$$

which can be combined with Eq (30) and rearranged to get

$$\frac{\mathbf{Z}_V + \mathbf{Z}'_1}{\mathbf{Z}_V}\left[1 + \frac{\mathbf{Z}_2}{\mathbf{Z}_2 + \mathbf{Z}'_1 + \mathbf{Z}_V}\right] = \frac{\mathbf{Z}_V}{\mathbf{Z}_V + \mathbf{Z}_{\rm in,fd}}. \tag{32}$$

This form makes it easy to estimate the effects of the fill capillary. When the fill-duct impedance is infinite, the right side vanishes and the previous resonance condition $\mathbf{Z}_V + \mathbf{Z}'_1 = 0$ is satisfied. When the right side is small but finite, the square brackets on the left side will have a magnitude near 2 because of the large magnitude of $\mathbf{Z}_2$. The first term on the left side equals the negative fractional perturbation in ω^2, which accordingly is

$$-\frac{\Delta\omega^2}{\omega^2} \approx \frac{\frac{1}{2}\mathbf{Z}_V}{\mathbf{Z}_V + \mathbf{Z}_{\rm in,fd}}. \tag{33}$$

In order to minimize the perturbation, the input impedance of the fill capillary must have a magnitude much larger than that of the chamber impedance. While it is possible to achieve this for short, capped ducts, the ducts required for filling and evacuating practical viscometers often have a length that is a significant fraction of a wavelength at the working viscometer frequency. In this case it is difficult to make the right side of Eq (33) negligible under a wide class of operating conditions (different gases, temperatures, pressures). These considerations led Wilhelm et al[2] to introduce a centered fill capillary.

The steady-state resonator response in Eq (27), modified to account for the fill capillary, is

$$p_2 = \frac{\mathbf{Z}_V\mathbf{Z}'_V\mathbf{Z}_2U_0}{(\mathbf{Z}'_1 + \mathbf{Z}'_V)(\mathbf{Z}_2 + \mathbf{Z}'_1 + \mathbf{Z}_V) + \mathbf{Z}_2(\mathbf{Z}'_1 + \mathbf{Z}_V)}. \tag{34}$$

This equation was used for analyzing data taken with the earlier versions of the viscometer.

E. Centered fill capillary

The current version of the viscometer has a fill capillary attached at the center of the main duct. The acoustic pressure has a node at this point for a symmetric resonator. This will minimize the coupling to the fill capillary, even for resonators with small asymmetries.

The modified viscometer is represented by the equivalent circuit in Fig 4. Each half of the original duct is now represented by a T-section. The impedance of the capillary duct, including end effects, is represented by $\mathbf{Z}_c$. The impedance $\mathbf{Z}'_a$ is the sum of the series term for a duct of length $L_d/2$ and the the end impedance at the chamber

$$\mathbf{Z}'_a = \mathbf{Z}_0 \tanh(\mathbf{\Gamma}L_d/4) + \mathbf{Z}_{\rm end}. \tag{35}$$

Similarly, the term

$$\mathbf{Z}''_a = \mathbf{Z}_0 \tanh(\mathbf{\Gamma}L_d/4) + \mathbf{Z}'_{\rm end} \tag{36}$$

includes a different end impedance, as appropriate for a junction of the fill capillary with the main duct. The other term in the T-sections is

$$\mathbf{Z}_b = \frac{\mathbf{Z}_0}{\sinh(\mathbf{\Gamma}L_d/2)}. \tag{37}$$

The circuit will have a low-frequency mode with $p_c = 0$

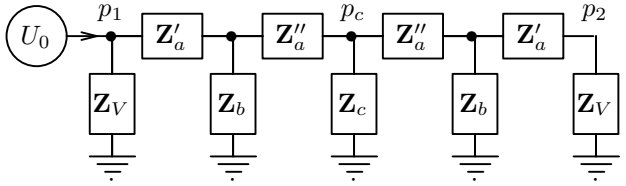

FIG. 4: Modified equivalent circuit with centered fill capillary represented by impedance $\mathbf{Z}_c$.

and $p_1 = -p_2$ if

$$\mathbf{Z}_V + \mathbf{Z}'_a + \frac{\mathbf{Z}_b \mathbf{Z}''_a}{\mathbf{Z}_b + \mathbf{Z}''_a} = 0. \tag{38}$$

After some manipulation this reduces to

$$\mathbf{Z}_1 + \mathbf{Z}_{\rm end} + \mathbf{Z}_V + \frac{\mathbf{Z}'_{\rm end}}{[\cosh(\mathbf{\Gamma} L_d/2) + \mathbf{Z}'_{\rm end}/\mathbf{Z}_b]\cosh(\mathbf{\Gamma} L_d/2)} = 0, \tag{39}$$

which is identical to Eq (23) when the impedance $\mathbf{Z}'_{\rm end} = 0$. This impedance has not been calculated; however it is proportional to a length on the order of the radius of the fill capillary, and thus should be negligible. It is kept in the following equations for completeness, but was set to zero when analyzing the data presented in this paper.

The output pressure p_2, obtained by solving the system of linear equations represented by Fig 4, is

$$p_2 = U_0 \frac{\mathbf{Z}_b^2 \mathbf{Z}_c \mathbf{Z}_V^2}{D_1 D_2}, \tag{40}$$

where

$$\begin{aligned} D_1 &= (\mathbf{Z}_b + \mathbf{Z}''_a)(\mathbf{Z}_V + \mathbf{Z}'_a) + \mathbf{Z}_b \mathbf{Z}''_a, \\ D_2 &= \mathbf{Z}_b \mathbf{Z}_V + 2\mathbf{Z}_c(\mathbf{Z}_b + \mathbf{Z}_V) \\ &\quad + \mathbf{Z}'_a(\mathbf{Z}_b + 2\mathbf{Z}_c) + \mathbf{Z}''_a(\mathbf{Z}_b + \mathbf{Z}_V + \mathbf{Z}'_a). \end{aligned}$$

Note that the vanishing of the denominator factor D_1 is equivalent to the resonance expression (38). Equation (40) is the theoretical resonance response function used in data analysis.

III. TESTS OF THE THEORY

The theory presented above was tested with data acquired using the resonator sketched in Fig 1. Measurements were taken on five well-studied gases: helium, argon, nitrogen, propane, and sulfur-hexafluoride. For these gases, the speed of sound, the thermal conductivity, and the viscosity are well known from independent measurements and, in the case of helium, even better known from theory.[13] The values of the resonator's physical dimensions used in the analysis of the data were determined by dimensional measurements and were not adjusted. The values of ϵ_i and ϵ_r were adjusted slightly to improve the quality of the fit to the helium data.

The test data were acquired over an interval of three weeks and span the pressure range 0.2 MPa to 3.2 MPa (For propane, the maximum pressure was 0.75 MPa, to avoid condensation.) At each value of the temperature and the pressure, the complex response function of the resonator was measured at 22 uniformly spaced frequencies spanning the range $\pm f/Q$ about center frequency f of the Greenspan mode. To do this, the frequency was set by a synthesizer and lock-in amplifiers were used to measure the complex voltage at the drive and detector transducers. We computed the complex ratio (detected voltage)/(drive voltage) at each frequency and fitted Eq (40) to the results. The main fitting parameters were D_v and the speed of sound c. The other fit parameters were a complex constant describing the proportionality of the complex voltage ratio to the acoustic pressure p_2 and a complex constant representing background coupling between the transducers. In some cases, a sloping background term was justified; this added an additional complex constant. The fits required values of the thermal diffusivity D_t and the specific heat ratio γ. For argon, nitrogen, propane and sulfur-hexafluoride, these quantities (as well as reference values of the speed of sound) were obtained from the database REFPROP[14]; for helium they were obtained from Refs 13, 15, and 16. Typically, the standard deviation of the voltage ratio from the fit was 0.02% of the maximum voltage. If the apparatus were fully understood, a fit of this quality could determine the viscosity with an uncertainty of 0.04%.

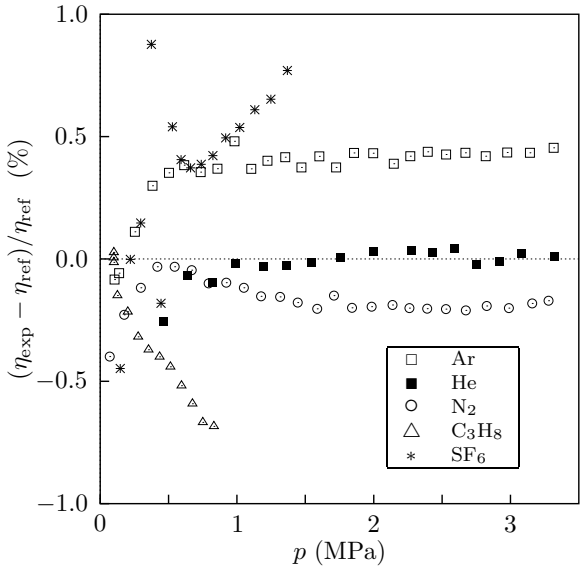

FIG. 5: Percentage differences between experimental viscosities and reference values for five gases, as functions of pressure.

In Fig 5, the resulting values of $\eta(p,T)$ are compared with reference values. For this critical comparison, we rescaled the values of $\eta(p,T)$ from the database REFPROP by the values of η_0 reported by Vogel and his collaborators. (Here, η_0 is the viscosity in the limit of

zero pressure at 298.15 K) In units of μPa·s, the values of η_0 are: nitrogen,[17] 17.782; argon,[17] 22.599; propane,[18] 8.155; sulfur hexafluoride,[19] 15.234. The reliability of the values of η_0 determined by Vogel *et al.* is confirmed by the agreement of their ratios with the ratios measured by Berg[20] (0.06% mean fractional difference) and by the small difference (0.13%) between their value of η_0 for helium (19.860)[17] and that calculated by Hurly and Moldover.[13]

The viscometer was tested over a wide frequency range. The resonance frequencies were 920 ± 30 Hz for helium, 326 ± 4 Hz for nitrogen, 295 ± 5 Hz for argon, 223 ± 7 Hz for propane, and 115 ± 6 Hz for sulfur-hexafluoride.

The argon viscosities differ from reference values by 0.4% at higher pressures. Both the helium and argon viscosities tend towards lower values at low pressures where sloping backgrounds were needed to get acceptable fits to the resonance profiles. Fits with constant background have the opposite trend at low pressures, tending towards higher viscosities. The viscosity of nitrogen is 0.2% below the reference values at high pressure and closer to the reference values at low pressure. The viscosities of propane and sulfur-hexafluoride are close to reference values at low pressure but differ significantly at higher pressures In these instances, we believe that the present results are more accurate than the reference data.

The properties of propane are representative of the polyatomic gases used in semiconductor processing. The sensitivity of the propane viscosity to the values of D_t needed for analyzing the data was tested by altering the input value of thermal conductivity by $\pm 10\%$; the corresponding changes in viscosity were $\mp 1\%$.

Figure 6 displays the deviations of the speeds of sound resulting from fitting the Greenspan viscometer data from reference values. The reference values were obtained from Ref 13 for helium, Ref 14 for argon and nitrogen, Ref 21 for propane, and Ref 22 for sulfur-hexafluoride. The results for helium, argon, and nitrogen within +0.01% to -0.03% of the reference values, and have similar, approximately linear dependences on pressure. This is surprisingly good for a resonator that was not designed to measure the speed of sound in gases. The poorer agreement of the propane and sulfur-hexafluoride results is consistent with the increasing uncertainty of the reference values as condensation is approached.

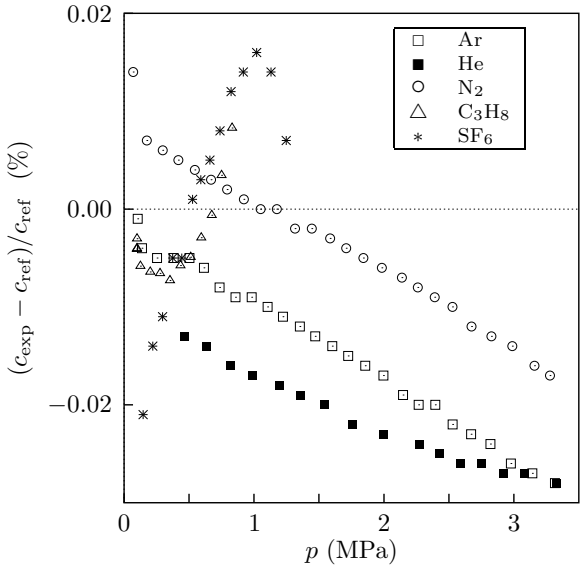

FIG. 6: Percentage differences between experimental speed of sound and reference values for five gases.

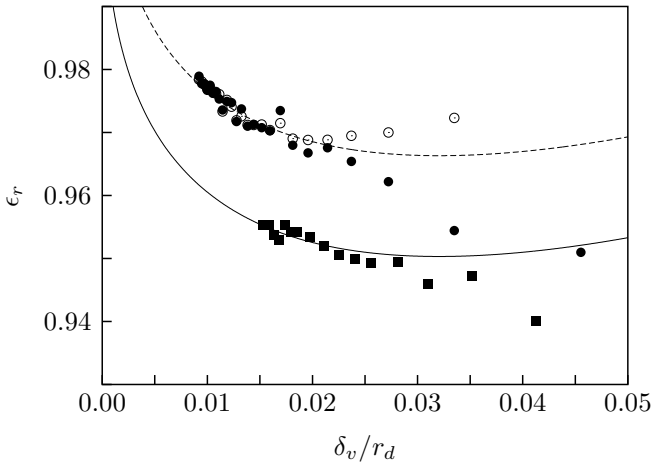

FIG. 7: Resistive end-effects parameter ϵ_r determined through fits to experimental data. ○, argon, constant background; ●, argon, sloping background; ■, helium, sloping background. The solid line is Eq (22) with $\epsilon_{r0} = 1.024$; the dashed line is Eq (22) with $\epsilon_{r0} = 1.04$.

APPENDIX A: FITS TO DETERMINE ϵ_r

The resistive end parameter ϵ_r was determined experimentally through fits to helium and argon data. For these fits, the viscous diffusivity was assumed known and ϵ_r was a free parameter. Figure 7 shows that the results have a weak, decreasing dependence on δ_v/r_d that is consistent with Eq (22). The coefficient $\epsilon_{r0} = 1.024$ chosen to fit the helium results was used for reduction of the data presented earlier in this paper.

APPENDIX B: SYMBOLS

$\mathbf{u}$ = acoustic velocity field
ρ = mass density
p = acoustic pressure
c = speed of sound
c_p (c_v) = heat capacity per unit mass at constant pressure (volume)
γ = c_p/c_v

$$
\begin{aligned}
A_d &= \pi r_d^2 = \text{ cross-sectional area of duct} \\
D_v &= \eta/\rho = \text{viscous diffusivity} \\
D_t &= \text{thermal diffusivity} \\
\delta_v &= \sqrt{2D_v/\omega} = \text{viscous penetration length} \\
\delta_t &= \sqrt{2D_v/\omega} = \text{thermal penetration length} \\
\kappa_v &= (1-i)/\delta_v \\
\kappa_t &= (1-i)/\delta_t \\
\mathbf{F}_v &= \frac{2J_1(\kappa_v r_d)}{\kappa_v r_d J_0(\kappa_v r_d)} \\
\mathbf{F}_t &= \frac{2J_1(\kappa_t r_d)}{\kappa_t r_d J_0(\kappa_t r_d)} \\
\mathcal{Z} &= \frac{i\omega\rho}{A_d}\,\frac{1}{1-\mathbf{F}_v} \\
\mathcal{Y} &= \frac{i\omega A_d}{\rho c^2}[1+(\gamma-1)\mathbf{F}_t] \\
\mathbf{Z}_0 &= \sqrt{\mathcal{Z}/\mathcal{Y}} \\
\mathbf{\Gamma} &= \sqrt{\mathcal{Z}\mathcal{Y}}
\end{aligned}
$$

All "small" acoustic quantities have an implicit time dependence proportional to $e^{i\omega t}$.

ACKNOWLEDGMENTS

This research was supported in part by the Office of Naval Research, by NASA under contract C-32088-K, and by the NIST Office of Microelectronics Programs. The authors thank Drs. J. J. Hurly and R. F. Berg for sharing data with us prior to their publication.

* keith.gillis@nist.gov
† jmehl@rockisland.com; 36 Zunuqua Trail, PO Box 307, Orcas, WA 98280-0307
‡ michael.moldover@nist.gov

[1] M. Greenspan and F. N. Wimenitz, "An Acoustic Viscometer for Gases-I," NBS Report 2658 (1953).
[2] J. Wilhelm, K. A. Gillis, J. B. Mehl, and M. R. Moldover, "An improved Greenspan Acoustic Viscometer," International Journal of Thermophysics, **21**, 983–997 (2000).
[3] M. R. Moldover K. A. Gillis, J. J. Hurly, J. B. Mehl, and J. Wilhelm. "Acoustic Measurements in Gases: Applications to Thermophysical Properties, Transport Properties, and and the Temperature Scale," in *Handbook of Elastic Properties of Solids, Fluids, and Gases*, (Academic Press, New York, 2000), Chap. 12.
[4] M. R. Moldover K. A. Gillis, J. J. Hurly, J. B. Mehl, and J. Wilhelm. "Acoustic Measurements in Gases," in *Modern Acoustical Techniques for the Measurement of Mechanical Properties*, M. Levy, H. E. Bass, and R. Stern, eds., (Academic Press, New York, 2001), 377–427.
[5] K. A. Gillis, J. B.Mehl, and M. R. Moldover, "Greenspan acoustic viscometer for gases," Rev. Sci. Instr. **67**, 1850–1857 (1996).
[6] P. M. Morse and K. Uno Ingard, *Theoretical Acoustics*, McGraw-Hill 1968, Sec. 6.4.
[7] The thermal term in the corresponding expression in References 2,3,5 was reduced by an incorrect factor of $2/\pi$. The correct formulation was, however, used for all data analysis.
[8] G. Kirchhoff, "Über den Einfluss der Wärmeleitung in einem Gase auf die Schallbewegung," Ann. Physik Chem. (Fifth Ser.) **134**, 177 (1868); English translation "On the Influence of Heat Conduction in a Gas on Sound Propagation," by R. B. Lindsay in *Benchmark Papers in Acoustics: Physical Acoustics*, R. B. Lindsay, Ed., (Dowden, Hutchinson, & Ross, Stroudsburg, Pennsylvania, 1974), p 7.
[9] I.B. Crandall, *Theory of vibrating systems and sound,* (Van Nostrand, New York, 1927), pp 229–241.
[10] See *e.g.* C.G. Montgomery, "Waveguides as Transmission Lines," *Principles of Microwave Circuits*, in C.G. Montgomery, R.H. Dicke, and E.M. Purcell, eds., (Dover, New York, 1965).
[11] J. B. Mehl, "Greenspan acoustic viscometer: Numerical calculations of fields and duct end effects," J. Acoust. Soc. Am. **106**, 73–82 (1999).
[12] J. B. Mehl, unpublished work.
[13] "*Ab initio* values of the thermophysical properties of helium as standards," John J. Hurly and Michael R. Moldover, J. Res. Natl. Inst. Stand. Technol. **105**, 667–688 (2000).
[14] E.W. Lemmon, M.O. McLinden, and M.L. Huber, "NIST Standard Reference Data Base 23: Reference Fluid Thermodynamic and Transport Properties, Version 7.0," National Institute for Standards and Technology, Standard Reference Data Program, Gaithersburg, MD, (2002).
[15] J. Kestin and W. Leidenfrost, "An absolute determination of the viscosity of eleven gases over a range of pressures," Physica **25**, 1033 (1959).
[16] J. Kestin, R. Paul, A. A. Clifford, and W.A. Wakeham, "Absolute determination of the thermal conductivity of the noble gases at room temperature up to 35 MPa," Physica A, **100**, 349–369 (1980).
[17] E. Vogel, "Präzisionsmessungen des Viskositätskoeffizienten von Stickstoff und den Edelgasen zwischen Raumtemperatur und 650 K," Ber. Bunsenges. Phys. Chem. **88**, 997 (1984).
[18] E. Vogel, C. Kuechenmeister, E. Bich, and A. Laesecke, "Reference correlation of the viscosity of propane," J. Phys. Chem. Ref. Data **27**, 947 (1988).
[19] T. Strehlow and E. Vogel, "Temperature dependence and initial density dependence of the viscosity of sulfur hexafluoride," Physica **A161**, 101 (1989).
[20] R. F. Berg, private communication.
[21] J. P. M. Trusler and M. P. Zarari, "The speed of sound in gaseous propane at temperatures between 225 K and 375 K and at pressures up to 0.8 MPa," J. Chem. Thermodynamics, **28**, 329–335 (1996).
[22] J. J. Hurly, D. R. Defibaugh and M. R. Moldover, "Thermodynamic Properties of Sulfur Hexafluoride," Int. J. Thermophys, **21**, 739–765, (2000).